INSTITUTE FOR FUSION STUDIES

DE-FG05-80ET-53088-717 IFSR #717-Review

Spectrum of Alfvén Waves, a Brief Review

S.M. MAHAJAN
Institute for Fusion Studies
The University of Texas at Austin
Austin, Texas 78712 USA
and
International Centre for Theoretical Physics
Trieste, Italy

September 1995

THE UNIVERSITY OF TEXAS

AUSTIN

Spectrum of Alfvén Waves, a Brief Review

by

S.M. MAHAJAN
The University of Texas at Austin
Austin, Texas
and
International Centre for Theoretical Physics
Italy

Abstract

Salient aspects of the Alfvén wave spectrum in hot confined plasmas are presented.

DISCLAIMER

Portions of this document may be illegible in electronic image products. Images are produced from the best available original document.

1 Introduction

The discoverer of the eponymous wave, Hannes Alfvén was a pioneer in the physics of charged fluids. The Alfvén wave,[1] in fact, is the very foundation on which the entire structure of magnetohydrodynamics (MHD) is erected. Beginning from a majestic original simplicity, it has acquired a rich and variegated character, and has ended up dictating most of the low-frequency dynamics of magnetized plasmas. This paper, a homage to Hannes Alfvén, is devoted to a discussion of the manifold manifestations of this wave of Alfvén.

Let us start with a brief recapitulation of the primeval wave propagating in a cold, infinite, homogeneous plasma embedded in a strong magnetic field $\mathbf{B_0}$. Within the framework of MHD, nontrivial wave motions occur if (the dispersion relation)

$$\left(\omega^2 - k_\parallel^2 v_A^2\right)\left(\omega^2 - k_\parallel^2 v_A - k_\perp^2 v_A^2\right) = 0 \tag{1}$$

where ω is the frequency, $k_\parallel = (\mathbf{k}\cdot\mathbf{B_0})/|\mathbf{B_0}|$ and $\mathbf{k}_\perp$ are respectively the wave numbers along and perpendicular to the ambient magnetic field $\mathbf{B_0}, v_A = |B_0|/(4\pi\rho)^{1/2}$ is the Alfvén speed, and ρ is the plasma density. In a homogeneous plasma, both $k_\parallel$ *and* $\mathbf{k}_\perp$ are good 'quantum numbers' and can be used to label the fluctuation, which in this case, can be either of $\mathbf{E}$, the electric field, $\mathbf{b}$, the perturbed magnetic field, or of the fluid displacement $\mathbf{v}$. The fluctuations, thus have the general form, $\boldsymbol{\mathcal{F}} = \sum_{\mathbf{k}} \boldsymbol{\mathcal{F}}_{k_\parallel,\mathbf{k}_\perp}\, e^{-i\omega t + i\mathbf{k}\cdot\mathbf{x}}$, with each $\boldsymbol{\mathcal{F}}_{k_\parallel,\mathbf{k}_\perp}$ evolving independently with a frequency $\omega = \omega(k_\parallel, \mathbf{k}_\perp)$ given by the dispersion relation (1). Naturally, the spectrum of the modes is continuous. For every ω, the dispersion relation is satisfied for some $k_\parallel$ *and* $\mathbf{k}_\perp$.

The simplest system allows two uncoupled independent modes:

(1) the shear mode, with the dispersion relation

$$\omega^2 = k_\parallel^2 v_A^2 \tag{2}$$

propagating along the ambient field and with its perturbed magnetic field $\mathbf{b}$ aligned perpendicular to $\mathbf{B}_0 (\mathbf{b} \cdot \mathbf{B}_0 = 0)$,

(2) and the compressible mode,

$$\omega^2 = k_\parallel^2 v_A^2 + k_\perp^2 v_A^2 \equiv k^2 v_A^2 \tag{3}$$

for which $\mathbf{b}$ is along $\mathbf{B}_0$.

Notice that the frequency of the shear wave (2) depends only on $k_\parallel$; this degeneracy of the shear wave with respect to $\mathbf{k}_\perp$ has profound consequences—it leads to a continuous spectrum[2-7] for the shear wave even in a bounded plasma. The principle focus of this paper will be on the determination of the spectra of the waves (2) and (3) in a variety of situations of physical interest.

Understanding of the Alfvénic motions is of utmost important in determining plasma stability as well as in proposing effective schemes pertaining to plasma heating and current drive. Vastness of the literature on the theory as well as applications of the Alfvén wave render it quite impossible to write an all encompassing review. The aim of the present review, therefore, is quite modest—it will focus on the spectral aspects of the wave. In that too, we shall concentrate primarily on what will be labeled 'Normally stable modes'; these are the modes which can become vehicles for plasma heating and current drive. The entire subject of stability of the Alfvén wave will be covered only qualitatively in the next subsection.

1.1 Stability

The dispersion relations (2) and (3) indicate that one can view $k_\parallel(k_\perp)v_A$ as the effective spring constants[7] of the plasma in response to a perturbation. Since a larger spring constant implies a greater ability of the plasma to maintain its state under external perturbations, the shear waves are more likely to go unstable as compared to the compressional waves $[k_\parallel < (k_\parallel^2 + k_\perp^2)^{1/2}]$. In most plasmas of interest, laboratory as well as astrophysical, $k_\perp^2 \simeq k^2 \gg k_\parallel^2$, tilting the instability balance further towards the shear wave.

It is small wonder then that most of the MHD stability literature is full of shear waves; kinks, sausages, pressure driven modes, etc. are all Alfvén waves of one variety or another. Where do these instabilities originate from? These naturally originate from 'nonthermal' features—which in this context—are inhomogeneities of all kinds: in density, in temperature, in the ambient magnetic field, in currents in the plasma... . The inhomogeneities complicate the plasma dynamics, and in the process, impart a rare richness to the Alfvén wave spectrum;[8–20] Alfvén waves in a curved and sheared magnetic field will display properties entirely unknown in the straight uniform field.

When various gradients are present, one could write (very schematically) the dispersion relation as

$$\omega^2 = \left\langle k_\parallel^2 v_A^2 \right\rangle - \left\langle \Delta^2 \right\rangle , \tag{4}$$

$$\Delta^2 = \Delta^2 \left[J_z, J_z', \kappa, p, \partial p/\partial x \cdots \right] ,$$

where Δ^2 represents the effects of the plasma current J_z, the current gradient (shear) J_z', the magnetic field curvature κ, the plasma pressure p; and the pressure gradient $\partial p/\partial x$. The symbol $\langle \quad \rangle$ stands for some appropriately weighted spatial average. Remembering that v_A^2 is generally large for a strongly magnetized plasma, the instability criterion ($\omega^2 < 0$)

$$\left\langle \Delta^2 \right\rangle > \left\langle k_\parallel^2 v_A^2 \right\rangle \tag{5}$$

can be satisfied only if $k_\parallel^2$ remains uniformly small in the region where the weighting function (the wave function) is finite; $k_\parallel \simeq 0$ is the region where the mode must be localized. Thus the modes localized around the $k_\parallel \simeq 0$ region (the flute-like modes) are the ones most likely to go unstable. Much of the MHD stability literature deals with modes of this nature. In recent years, additional driving mechanisms like a species of fast particles (to simulate hot fusion generated alpha particles in a reactor) are often included in stability theory.

Barring a few exceptional cases (when strong external drives are present), the normal plasma cannot come up with a sufficient $\langle \Delta^2 \rangle$ to overcome $\left\langle k_\parallel^2 v_A^2 \right\rangle$ if $k_\parallel$ is finite everywhere.

These normally stable modes are of great importance. Just as the unstable modes transfer energy from the plasma to the electromagnetic (e.m.) fields, the stable modes are a channel for transferring energy from the external fields to the plasma. Thus for applications like plasma heating, one must turn to the intrinsically stable modes.

In Sec. 2, the simplest cylindrically symmetric model for a cold plasma is introduced, and the model is investigated to delineate the general nature of the shear Alfvén spectrum. Section 3 is devoted to a similar discussion of the compressional mode. In Sec. 4, the equilibrium geometry is generalized to two dimensions leading to the emergence of gap modes; it is shown that nonsingular normalizable eigenfunctions are possible for these modes. In Sec. 5, a few qualitative summary remarks are presented.

2 Cylindrical Plasma

In this section we shall study the Alfvén waves (unless stated otherwise, the Alfvén wave will denote that branch of the dispersion relation which reduces to $\omega = k_\parallel v_A$ in the infinite homogeneous limit) in a cylindrical confined plasma. Keeping in mind that many of our considerations are intended for large aspect ratio toroidal systems [fusion devices, coronal rings...], we shall view the cylinder as an approximation of a theorist's thin torus. Thus we deal with an opened-up torus—which is really a cylinder of length $2\pi R$, R being the major radius of the torus. In this paper only the toroidally (axially) symmetric equilibria will be considered; the direction $\xi(z/R)$ will always be ignorable. In much of this paper we will further assume that the plasma equilibrium is also poloidally (azimuthally) symmetric—is independent of the angle θ.

2.1 Basic Equations

We deal with Alfvén waves (with arbitrary $k_\parallel$) propagating in an inhomogeneous current-carrying low β plasma. The basic equations will include electron parallel dynamics—an effect

of great importance in removing the MHD singularity. Complications arising from finite ion temperature will be ignored. We reproduce here the set of equations used in Refs. 9-11; the reader may consult the original work and the references therein for details concerning their derivation.

One begins with the radial and perpendicular components of Ampére's law [perpendicular here means the direction on the magnetic surface perpendicular to the field line. The orthogonal system consists of $\hat{\mathbf{e}}_\parallel = \hat{\mathbf{b}} = \mathbf{B}_0/|\mathbf{B}_0|$, $\hat{\mathbf{r}}$, and $\hat{\mathbf{e}}_\perp = \hat{\mathbf{b}} \times \hat{\mathbf{r}}$]

$$(F - k_\perp^2)E_r = i\left(\frac{k_\perp}{r}\frac{d}{dr}r - (S + A)\right)E_\perp + ik_\parallel E_\parallel' + i\left[\frac{(r\delta)'}{r}\right]k_\perp E_\perp, \tag{6}$$

and

$$\left(F + \frac{d}{dr}\frac{1}{r}\frac{d}{dr}r\right)E_\perp = i\left(\frac{d}{dr}k_\perp + S + A\right)E_r - k_\parallel k_\perp E_\parallel - 2\delta' E_\parallel' + \left(\frac{\delta}{r^2}\right)E_\parallel - \left[\frac{(r\delta')}{r}\right]E_\parallel, \tag{7}$$

where $E_r, E_\perp$, and $E_\parallel$ are respectively the radial, perpendicular and parallel components of the wave electric field, the prime ($'$) denotes differentiation with respect to r, and

$$F = \alpha_1\left(\frac{\omega^2}{v_A^2}\right) - k_\parallel^2, \tag{8}$$

with $\alpha_1 = (1 - \omega^2/\omega_{ci}^2)^{-1}$ and $S = (\alpha_1\omega^2/v_A^2)(\omega/\omega_{ci})$ representing finite ω/ω_{ci} effects, and

$$A = \left[\frac{1}{r}(1 + \delta^2)\right]\left(-2k_\parallel\delta + k_\perp\delta^2\right) \tag{9}$$

is due to the presence of the parallel current in the plasma. The parallel current produces a poloidal magnetic field B_p, and manifests itself through $\delta \simeq B_p/B_0 = r/Rq \ll 1$, where q is the safety factor. The parallel current also modifies the wavenumbers, which are defined by

$$(1 + \delta^2)^{1/2}k_\parallel = -\frac{l}{R} + \frac{m}{qR} = -\frac{l}{R} + \frac{m}{r}\delta, \tag{10}$$

$$(1 + \delta^2)^{1/2}k_\perp = \frac{m}{r} - \frac{l}{R}\delta, \tag{11}$$

where l and m are the toroidal and poloidal numbers respectively [$\mathbf{E}(\mathbf{x}) = \mathbf{E}(r)\,e^{-im\theta + il(z/R)}$].

Notice that in Eqs. (6) and (7), we have retained only the leading terms containing $E_\parallel$. This is justified because the parallel electric field for Alfvén waves is much smaller than the perpendicular fields $E_\perp$ and E_r. We can readily eliminate E_r between Eqs. (6) and (7) to obtain a rather complicated equation relating $E_\perp$ and $E_\parallel$. Considerable simplification is achieved by assuming that $\omega/\omega_{ci} < \delta \ll 1$, and $k_\perp^2 \equiv m^2/r^2 > k_\parallel^2 < \omega^2/v_A^2$, and retaining terms only to $\mathcal{O}(\delta)$. Neither of these assumptions is particularly restrictive. Within the context of the above mentioned approximations, we can derive a relatively simple equation [see Ref. 11]

$$\left[F - \frac{d}{dr}\frac{F}{rk_\perp^2}\frac{d}{dr}r\right]E_\perp + gE_\perp = \frac{k_\parallel}{rk_\perp}\left[\frac{d}{dr}r\frac{dE_\parallel}{dr} - rk_\perp^2 E_\parallel\right], \tag{12}$$

where

$$g = \frac{(S+A)'}{k_\perp} + \frac{(S+A)^2}{k_\perp^2}, \tag{13}$$

represents the combined effect of the equilibrium current and finite ω/ω_{ci}.

We would like to point out here that if $E_\parallel$ is neglected, Eq. (12) becomes the standard MHD equation, with $F = 0$ as its singular point leading to the well-known continuum. This equation has been extensively studied. With $E_\parallel$ included, we need one more equation relating $E_\perp$ and $E_\parallel$ to complete the system. For this purpose, we could use either the parallel component of Ampére's law, or the quasineutrality condition $\nabla \cdot \mathbf{J} = 0$, where $\mathbf{J}$ is the perturbed current. In this paper, we use the latter condition, which is [see Refs. 9, 11]

$$ik_\parallel \frac{\zeta}{k_\parallel^2\rho_s^2}E_\parallel + \frac{v_A^2}{r}\frac{d}{dr}\frac{r}{v_A^2}\left(E_r + i\frac{\omega}{\omega_{ci}}E_\perp\right)$$

$$+ik_\perp\left(E_\perp - i\frac{\omega}{\omega_{ci}}E_r\right) = 0, \tag{14}$$

where $\rho_s = c_s/\omega_{ci} = (T_e/m_i)^{1/2}/\omega_{ci}$ is the ion gyroradius with electron temperature T_e. For all cases of interest in this study, $k_\parallel^2\rho_s^2 \ll 1$ implying that the parallel wave length of the mode is much larger than the effective gyroradius.

In Eq. (14), ζ is the collisionless parallel electron response,

$$\zeta = 1 + \frac{\omega}{|k_\parallel| v_e} Z\left(\frac{\omega}{|k_\parallel| v_e}\right), \tag{15}$$

where Z is the plasma dispersion function, and $v_e = (2T_e/m_e)^{1/2}$ is the electron thermal speed. For most hot plasmas of interest, the collisionless assumption for Alfvén waves is quite valid. For small l and m numbers, the typical wave frequency $\omega \sim 10^7 \gg \nu \sim< 10^5$, where ν is the collision frequency. However, it is quite straightforward to calculate parallel electron response using a particle conserving Krook collisional operator. The resulting expression for ζ is

$$\zeta = 1 + \frac{\omega + i\nu}{|k_\parallel| v_e} Z\left(\frac{\omega + i\nu}{|k_\parallel| v_e}\right) \times \left[1 + \frac{i\nu}{|k_\parallel| v_e} Z\left(\frac{\omega + i\nu}{|k_\parallel| v_e}\right)\right]^{-1}, \tag{16}$$

which reduces to Eq. (15) for $\nu = 0$. Thus making use of Eq. (16) for ζ allows us to deal with a collisional plasma as well. Note that in deriving Eq. (16), we have neglected the effects of the parallel current, which will doppler shift ω to $\omega - k_\parallel v_d$, where v_d is the electron drift speed. This is justified because $\omega \simeq k_\parallel v_A \gg k_\parallel v_d$, because $v_d \ll v_A$. The effect can be retained without complicating the analysis. We would like to point out that in the strongly collisional limit ($\nu \gg \omega, |k_\parallel| v_e$), Eqs. (14) and (16) simply reduce to one of the equations of resistive magnetohydrodynamics; the temperature dependence in ρ_s^2 exactly cancels the temperature dependence in the expanded Z-functions.

To eliminate E_r between Eqs. (6) and (14), we first rewrite Eq. (6) in the approximate form ($F \ll k_\perp^2$),

$$E_r = -i\left(\frac{1}{rk_\perp}\frac{d}{dr}r - \frac{1}{k_\perp^2}(S + A)\right) E_\perp - i\frac{k_\parallel}{k_\perp^2} E_\parallel' - i\frac{(r\delta)'}{rk_\perp} E_\parallel, \tag{17}$$

and then substitute Eq. (17) into Eq. (14) to yield

$$k_\parallel \frac{\zeta}{k_\parallel^2 \rho_s^2} E_\parallel - \frac{1}{r}\frac{d}{dr} r\left(\frac{k_\parallel}{k_\perp^2} E_\parallel' + \frac{(r\delta)'}{rk_\perp} E_\parallel\right) = \frac{1}{rk_\perp}\left(\frac{1}{r}\frac{d}{dr} r \frac{d}{dr} r - k_\perp^2\right) E_\perp \tag{18}$$

where only the leading order terms have been retained on the right-hand side. Since $E_\parallel$ is small, it is sufficient to determine it to leading order. On the left side of Eq. (18), the terms

in the square brackets are small compared to the first term because $d/dr \sim k_\perp$, $\zeta < 1$, and $k_\parallel^2 \rho_s^2 \ll 1$. Therefore, Eq. (18) simplifies to

$$E_\parallel \simeq \frac{k_\parallel}{k_\perp} \frac{\rho_s^2}{\zeta} \left(\frac{1}{r^2} \frac{d}{dr} r \frac{d}{dr} r - k_\perp^2 \right) E_\perp, \tag{19}$$

and, when substituted into Eq. (12), it gives the required fourth order equation

$$\left(F - \frac{d}{dr} \frac{F}{r k_\perp^2} \frac{d}{dr} r \right) E_\perp + g E_\perp = \frac{k_\parallel}{r k_\perp} \left[\frac{d}{dr} r \frac{d}{dr} - r k_\perp^2 \right) \frac{k_\parallel}{k_\perp} \frac{\rho_s^2}{\zeta} \times \left(\frac{1}{r^2} \frac{d}{dr} r \frac{d}{dr} r - k_\perp^2 \right) E_\perp \tag{20}$$

which describes Alfvén waves in an inhomogeneous, current-carrying, cylindrical plasma. Due to the presence of the fourth order term $F = 0$ is no more a singular point of the differential equation. It must also be stated that Eq. (20) is relatively exact; the only approximations made are 1) $k_\perp^2 > k_\parallel^2 \sim \omega^2/v_A^2$, and 2) $k_\parallel^2 \rho_s^2 \ll 1$. The latter automatically guarantees $E_\parallel/E_\perp \ll 1$ [see Eq. (19)] and the former condition $\omega \sim k_\parallel v_A (F \simeq 0)$ simply defines the domain of the shear Alfvén wave. However, the effects of compression (magnetic field compression) have not been neglected in deriving Eq. (20). In fact, in an inhomogeneous plasma, the shear and the compressional modes are coupled, and an adequate description of Alfvén waves requires the presence of both the polarizations. If $\omega \sim k_\parallel v_A$, then the compressional wave is evanescent with the WKB dispersion relation $k_r^2 + k_\perp^2 = 0$. Thus the Alfvén waves, even in this frequency range, are some linear combination of the two modes of the homogeneous plasma; the shear and the compressional, and Eq. (20) correctly describes the situation.

We end this section by remarking that Eq. (20) can also be used to study the tearing modes in a current carrying compressible plasma.

2.2 Eigenmode Equation

We are interested in investigating the nature of Alfvén waves in the frequency range given by $F \simeq 0$ or $\omega \simeq k_\parallel v_A$. It is clear that $F = 0$ is no more a singular point of the differ-

ential equation implying that the logarithmically singular solutions, which constitute the MHD continuum, are no more there. For general temperature, current, and density profiles, Eq. (20) should be solved numerically. Most of the important and interesting features of this system, however, can be illustrated by studying the system where the profile of $k_\parallel^2 v_A^2$ has a minimum at a point $r = r_0 \neq 0$ in the plasma. Thus, the analysis excludes the cases for which $k_\parallel^2 v_A^2$ has a minimum at $r = 0$, the plasma center. However, we expect all the general results to be essentially valid even for this case.

Since the modes of interest are characterized by $F \simeq 0$, we carefully expand F around the point r_0, the minimum of $k_\parallel^2 v_A^2$, i.e.,

$$\left(k_\parallel^2 v_A^2\right)'_{r_0} = 0, \tag{21}$$

because F is a rapidly varying function in the vicinity of r_0. All other quantities in the differential Eq. (20) will be evaluated at $r = r_0$. Within the context of the preceding discussion, it is straightforward to show that Eq. (20) can be cast in the form

$$\frac{d}{dy}(y^2 - \mu)\frac{dE_\perp}{dy} - k_\perp^2 a^2 (y^2 - \mu) E_\perp + g_0 E_\perp = \overline{\sigma}\left(\frac{d^2}{dy^2} - k_\perp^2 a^2\right)^2 E_\perp, \tag{22}$$

where the new variable y is displaced from $r - r_0$, and is given by

$$y = \frac{r - r_0}{a} + \frac{F_0}{2\Lambda^2}\frac{a}{L_n}$$

where a is the radius of the cylinder, $F_0 = F(r = r_0)$, $L_n^{-1} = (n^{-1}dn/dr))_{r=r_0}$, the density gradient scale length at $r = r_0$, $\Lambda^2 = -(a^2/2)(F'')_{r=r_0}$ and

$$\mu = \frac{F_0}{\Lambda^2}\left(1 + \frac{1}{4}\frac{F_0}{\Lambda^2}\frac{a^2}{L_n^2}\right) \tag{23}$$

is the effective eigenvalue to be determined. In the rest of this section, all quantities, unless otherwise stated are to be evaluated at $r = r_0$. For modes under consideration $F_0/\Lambda^2 \ll 1$, making $\mu \simeq F_0/\Lambda^2$, and $y \simeq (r - r_0)/a$. In Eq. (22), $k_\perp = (k_\perp)_{r=r_0} = m/r_0$ is the poloidal

mode number, $g_0 = (k_\perp^2 a^2/\Lambda^2)(g)_{r=r_0}$, and

$$\overline{\sigma} = \left(\frac{k_\parallel^2}{\Lambda^2}\frac{\rho_s^2}{a^2}\frac{1}{\zeta}\right)_{r=r_0} \tag{24}$$

is the measure of the non MHD effects; in this case the effect of electron parallel dynamics. Notice that $\overline{\sigma}$ will be generally complex. For $\overline{\sigma} = 0$, Eq. (22) reduces to the extensively studied MHD equation with ω/ω_{ci} effects, etc. In this case, it is clear that for $\mu > 0$ ($F_0 > 0$) the equation is singular, and leads to the MHD continuum. For $\mu < 0$, however, there is no singularity, and the discrete spectrum of marginally stable global Alfvén waves (GAE) emerges. With the inclusion of the non-MHD effects ($\overline{\sigma} \neq 0$), the picture changes, and a new discrete spectrum encompassing the continuum and the GAE results. From Eq. (24), it appears that $\overline{\sigma} \to 0$ for $k_\parallel \to 0$ making Eq. (20) unsuitable for modes with $k_\parallel \simeq 0$ (also a minimum of $k^2 v_A^2$). However, as $k_\parallel \to 0$, $\zeta \to k_\parallel^2$. Therefore $\overline{\sigma}$ remains finite, and Eq. (20) can deal with this subclass of modes ($k_\parallel \simeq 0$).

Equation (22) is best analyzed in the Fourier space. Defining

$$E = \frac{1}{(2\pi)^{1/2}}\int_{-\infty}^{+\infty} dy E_\perp \exp(iyp),$$

$$E_\perp = \frac{1}{(2\pi)^{1/2}}\int_{-\infty}^{+\infty} dp E \exp(-iyp), \tag{25}$$

we obtain

$$\frac{d}{dp}\left(p^2 + k_\perp^2 a^2\right)\frac{dE}{dp} + \left[\mu(p^2 + k_\perp^2 a^2) + g_0 - \sigma(p^2 + k_\perp^2 a^2)^2\right] E = 0, \tag{26}$$

which becomes

$$\frac{d}{dx}\left(1 + x^2\right)\frac{dE}{dx} + \left[\epsilon(1 + x^2) + g_0 - \sigma(1 + x^2)\right] E = 0 \tag{27}$$

where $\epsilon = k_\perp^2 a^2 \mu, \sigma = k_\perp^4 a^4 \sigma$, and $p = k_\perp a x$. We can further transform Eq. (26) using a new dependent variable

$$\psi = (1 + x^2)^{1/2} E, \tag{28}$$

to yield the Schrödinger equation

$$\frac{d^2\psi}{dx^2} + (\epsilon - V(x))\psi = 0, \tag{29}$$

where $\epsilon = \mu k_\perp^2 a^2$ is the eigenvalue, and

$$V(x) = -\frac{g_0}{1+x^2} + \frac{1}{(1+x^2)^2} + \sigma(1+x^2), \tag{30}$$

is the effective potential.

2.3 General Features

An examination of the effective potential $V(x)$ [Eq. (30)] appearing in the mode Eq. (29) yields a wealth of information about the nature of the eigenmodes. To maintain continuity with the published literature, we again begin with the MHD limit $\sigma = 0$. In Fig. 1, we have plotted $V(x)$ as a function of x for several values of g_0. It is straightforward to see:

1) For $g_0 \leq 0$, $V(x)$ is a monotonically decreasing function of x, resulting in an effective potential hill at $x = 0$. Thus no localized eigenmodes around $x = 0$ are possible for any ϵ. Only the continuum modes exist.

2) For $g_0 \geq 2$, $V(x)$ has a minimum at $x = 0$ [$V(0) = -g_0 + 1$], and approaches zero as x^{-2} as x goes to infinity implying a potential well at $x = 0$. Since the potential $V(x)$ is negative everywhere, the equation $\epsilon - V(x) = 0$, has real solutions if and only if $\epsilon < 0$. Thus, the real turning points, and hence the bound states exist only for $\epsilon < 0$. This is the discrete spectrum of GAE. Details for this case can be seen in Ref. 10. Since there are no real turning points for $\epsilon \geq 0$, there are no bound states, and only a continuum prevails; $\epsilon = 0$ defines the lower edge of this well-known shear Alfvén continuum,

3) For $0 < g_0 < 2$, $V(x)$ has considerably more structure with a maximum at $x = 0$ and two minima at $x = \pm[(2/g_0) - 1]^{1/2}$. Clearly for $\epsilon \geq 0$, no bound states are possible. This proves that regardless of the value of g_0, $\epsilon \geq 0$ always corresponds to the continuum modes.

In this range of g_0, it is a little hard to determine the criterion which allows the existence of discrete modes for $\epsilon < 0$. The question has been dealt with in detail in Refs. 10, 13, where it is shown that $g_0 > (1/4)$ is required for the discrete spectrum to be possible. The reason is, that although minima of the potential exist, they are not deep enough to contain a mode.

Figure 2 contains plots of $V(x)$ versus x for several values of g_0, and for a finite but small value of $\sigma \simeq 10^{-2}$. We have chosen σ to be real for simplicity. The general nature of the following discussion will hold for a realistic complex σ.

There are several features which distinguish Fig. 2 from Fig. 1 ($\sigma = 0$). The most important is the behavior of $V(x)$ as $x \to \infty$. While for $\sigma = 0$, $V(x) \to 0$ as $x \to \infty$, for finite σ, $V(x) \to x^2$. For large x, the potential is like that of a simple harmonic oscillator and implies bound states for all values of g_0, because the equation $\epsilon - V(x) = 0$ always has real solutions. Thus the erstwhile MHD continuum for $\epsilon \geq 0$, has changed over to a discrete spectrum, to that of the Kinetic Alfvén Wave[21] (KAW). Depending upon the value of g_0, the lowest eigenmode may be characterized by an eigenvalue $\epsilon < 0$. Thus, the distinction between GAE and the continuum has disappeared. They are the parts of the same discrete spectrum; the lowest eigenvalue will be positive or negative depending upon the value of g_0, which is due to the presence of equilibrium currents and ω/ω_{ci} effects.

From Fig. 2, it is also obvious that for positive g_0, the lowest mode will be localized in the potential well around $x = 0$, and will not sample the form of the potential for large x. Thus its character is only mildly affected by the presence of σ. Since σ is due to the dissipative processes (for example, Landau damping for a collisionless case), the mode will have very slight damping.

The case for $g_0 \leq 0$ is altogether different. Since these modes are formed because of the turning points at large x (due to the term proportional to σ), their mode structure as well as the eigenvalue strongly depends upon σ. As a result, these modes are considerably more damped.

We remind the reader that Eqs. (28) and (29) are in the Fourier space x. The real spatial variable is $y \simeq (r - r_0)/a$. Since $p = k_\perp a x$ and y are conjugate Fourier variable, $k_\perp a \Delta x \Delta y \sim 1$, where Δx and Δy are respectively the widths in x and y. Therefore, the GAE modes, (now corresponding to the lowest modes for certain values of g_0) which are narrow in x, are relatively broad in y, possibly extending over most of the plasma. This justifies their name, Global Alfvén Eigenmodes. The exact width, however, is a function of the m number; $\Delta r \simeq r_0/|m|$, and can become quite small if $|m| \gg 1$. The discrete modes lying in the MHD continuum, however are comparatively broad in x (because of the smallness of σ), and therefore narrow in y. Thus, in real space, these modes are strongly localized around $r \simeq r_0(y = 0)$. This is to be expected, because for $\sigma = 0$, these modes were logarithmically singular at $F = 0$ ($y = 0$), and the presence of σ has simply spread the singularity in a finite region around $y = 0$, resulting in finite amplitude everywhere.

2.4 Alfvén Wave Spectrum—A Variational Calculation

The mode equation (Eq. (29) can be readily solved by numerical integration to obtain exact eigenvalues and eigenfunctions. In the present review, however, we present approximately analytic dispersion relations using a variety of techniques, in particular, the variational technique, which is warranted by the self-adjoint character of Eq. (27) or (29).

Although Eq. (29) was more useful in delineating the general features of the system, Eq. (27) is more suitable for a variational treatment. The functional $\left[\langle \quad \rangle \equiv \int_{-\infty}^{+\infty} dx\right]$,

$$S = -\left\langle (1+x^2)(E_p')^2 \right\rangle + \left\langle \left[\epsilon(1+x^2) + g_0 - \sigma(1+x^2)^2\right] E_p^2 \right\rangle \tag{31}$$

is variational in the sense that $\delta S = 0$ reproduces the Euler equation (27). In addition, the extremal value of $S = 0$.

Equation (31) can be used to obtain an eigenvalue by choosing a trial function with a variational parameter. The eigenvalue obtained will correspond to a radial mode number

equal to the number of nodes (zeros) of the trial function. The variational calculation can become quite involved for higher radial mode numbers. Therefore, we limit ourselves to the lowest eigenmode, and choose a trial function with no zeros for finite x,

$$E_p = e^{-\alpha x^2/2}\,, \mathrm{Re}\;\alpha > 0. \tag{32}$$

Substituting Eq. (32) into Eq. (31), and carrying out the integrals, we find

$$S \propto \left(\epsilon - \sigma + g_0 - \frac{3}{4}\right) - \frac{\alpha}{2} + (\epsilon - 2\sigma)\frac{1}{2\alpha} - \frac{3\sigma}{4}\frac{1}{\alpha^2}. \tag{33}$$

To find ϵ and α, we must simultaneously solve the equations $S = 0$, and

$$\frac{\partial S}{\partial \alpha} = 0 = -\frac{1}{2} - \frac{(\epsilon - 2\sigma)}{2\alpha^2} + \frac{3}{2}\frac{\sigma}{\alpha^3}. \tag{34}$$

An examination of Fig. 2 is helpful in making progress. Evidently, for $g_0 \gtrsim 2$, there is a potential well at $x = 0$, and the lowest mode is expected to be a GAE, essentially confined in this well with a negative eigenvalue $\epsilon = -|\epsilon|$. Further, the size of the well is $\Delta x \sim 1$ implying that $\alpha \simeq 1$. In this case, Eq. (34) gives ($\sigma \ll 1$)

$$\alpha = (2\sigma - \epsilon)^{1/2} = [2\sigma + |\epsilon|]^{1/2}. \tag{35}$$

Substituting Eq. (35) into the equation $S = 0$, correct to order σ, we obtain

$$\epsilon = -|\epsilon_0| + \frac{2|\epsilon_0| + 2|\epsilon_0|^{1/2} + 1.5}{2|\epsilon_0| + |\epsilon_0|^{1/2}}\,\sigma \equiv -|\epsilon_0| + \tau\sigma \tag{36}$$

where

$$\epsilon_0 = g_0 - \frac{1}{4} - \left(g_0 - \frac{1}{2}\right)^{1/2} \tag{37}$$

is the MHD result, and the terms proportional to σ are small correction to the eigenvalue. To show that Eq. (36) implies weak Landau-damping, let us evaluate σ for the collisionless hot plasma case. The definition of a hot plasma,[9] in the present context, is that at $r = r_0$, $\omega < k_\parallel v_e$ which leads to $(\zeta)^{-1} \simeq 1 - i\pi^{1/2}(\omega/k_\parallel v_e)$, and

$$\sigma = (k_\perp a)^4 \frac{k_\parallel^2 \rho_s^2}{a^2 \Lambda^2}\left(1 - i\sqrt{\pi}\,\frac{v_A}{v_e}\right), \tag{38}$$

where we have used $\omega < k_\parallel v_A$ in the damping term. Substituting Eq. (38) into Eq. (36), and making use of the definition of ϵ, we obtain

$$\alpha_1\left(\frac{\omega^2}{v_A^2}\right) = k_\parallel^2\left[1+\tau k_\perp^2\rho_s^2\left(1-i\pi^{1/2}\frac{v_A}{v_e}\right)\right] - \frac{\epsilon_0\Lambda^2}{k_\perp^2 a^2} \tag{39}$$

Notice that σ corrections have led to a change in the real part of the frequency in addition to the damping. From Eq. (39), it is straightforward to show that

$$\frac{\text{Im }\omega}{\text{Re }\omega} = -\frac{\tau}{2}\,k_\perp^2\rho_s^2\pi^{1/2}\,\frac{v_A}{v_e}. \tag{40}$$

Thus Eqs. (39) and (40) are the dispersion relation for the lowest radial eigenmode for the case $g_0 \gtrsim 2$. These are the mildly damped GAE.

The width of the trial function is equal to $(2/\alpha)^{1/2} = (2)^{1/2}|\epsilon|^{-1/4}$ [Eqs. (32) and (35)]. Thus $\Delta y = (k_\perp a)^{-1} \simeq (k_\perp a)^{-1}|\epsilon|^{1/2}(2)^{-1/2}$ is of order unity for low-m numbers, implying that the mode is radially broad, and covers a large part of the plasma.

In the range $1/4 < g_0 < 2$, the lowest eigenmode still should be a GAE, however the structure of the potential is complicated enough that Eq. (37)–(39) can only be qualitatively correct. The accuracy can be improved by using more involved trial functions, but the procedure turns out to be tedious and not very illuminating. For quantitatively correct results in this range, one must depend upon numerical solutions.[9]

For values of $g_0 < 1/4$, there were no bound states for $\sigma = 0$ (continuum modes). In this range, it is the σ dependent terms that provide the confining potential even for the lowest eigenmode. It was discussed in Sec. 2.2 that these modes are broad in x (narrow in real space), suggesting that we seek a solution of Eq. (33) and (34) for $\alpha \ll 1$. Approximate solutions are

$$\alpha = \frac{3\sigma}{\epsilon - 2\sigma}, \tag{41}$$

and

$$\epsilon \simeq \left(1-\frac{4}{3}g_0\right)^{1/2} 3\sigma^{1/2} + 2\sigma \simeq \left(1-\frac{4}{3}g_0\right)^{1/2} 3\sigma^{1/2} \tag{42}$$

because $\sigma \ll 1$. Thus we already see that the eigenvalue turns out to be proportional $\sigma^{1/2}$ in contradistinction to the case $g_0 > 2$, where the changes in the eigenvalue were proportional to σ. Since σ is the measure of the damping, these kinetic modes (which were in the continuum) are much more damped as compared to the GAE. We can rewrite Eq. (42) in the form

$$\alpha_1 \left(\frac{\omega^2}{v_A^2}\right) = k_\parallel^2 \left[1 + \left(1 - \frac{4}{3} g_0\right)^{1/2} 3 \left|\frac{\Lambda}{k_\parallel}\right| \frac{\rho_s}{a} \left(1 - \frac{i\pi^{1/2}}{2} \frac{v_A}{v_e}\right)\right] \tag{43}$$

from which we deduce

$$\begin{aligned} \frac{\mathrm{Im}\,\omega}{\mathrm{Re}\,\omega} &\simeq -\left(1 - \frac{4}{3} g_0\right)^{1/2} \frac{3}{2} \left|\frac{\Lambda}{k_\parallel}\right| \frac{\rho_s}{a} \frac{\pi^{1/2}}{2} \frac{v_A}{v_e} \\ &= -\left(1 - \frac{4}{3} g_0\right)^{1/2} \frac{3}{4} \left|\frac{\Lambda}{k_\parallel}\right| \left(\frac{\pi}{2}\right)^{1/2} \frac{c}{a\omega_{pe}} \end{aligned} \tag{44}$$

where c is the speed of light in vacuum, and $\omega_{pe} = (4\pi n_0 e^2/m_e)^{1/2}$ is the electron plasma frequency. Thus we notice that the damping of the erstwhile continuum modes (KAW) is independent of electron temperature to leading order. It is nonzero as long as the effects of finite electron mass are retained. It is, of course, of utmost importance to realize that the discrete spectrum is also contingent upon finite electron inertia, otherwise the system relapses to the MHD shear Alfvén continuum. Equation (44) clearly shows why the damping of the continuum modes is essentially independent of the model for describing electron parallel dynamics. The radial width of this mode can be computed using Eqs. (37) and (41), and is

$$\Delta y = \frac{r - r_0}{a} = \left(\frac{k_\parallel^2 \rho_s^2}{\Lambda^2 a^2}\right)^{1/4} \simeq \left(\frac{\rho_s}{a}\right)^{1/2} \ll 1. \tag{45}$$

2.5 Higher Radial Eigenmodes

Although for most practical applications (for example, the Alfvén wave heating or current drive), the lowest radial eigenmode of Alfvén waves (whether a GAE, or the continuum kind) is important, it is of some interest to calculate the higher radial eigenmodes. The reader is referred to Ref. 9 for a calculation for the GAE's ($\sigma = 0$). We concentrate here on the case

when $g_0 \lesssim 1$, and solve Eq. (29) for higher radial mode numbers. Since the turning points of the equation are determined by the term proportional to σ, we choose to solve the simplified simple harmonic oscillator equation

$$\psi'' + [\epsilon - \sigma - \sigma x^2]\psi = 0, \tag{46}$$

which has a spectrum

$$\epsilon_n = \sigma + (2n+1)\sigma^{1/2} \simeq (2n+1)\sigma^{1/2}, \tag{47}$$

where n is the radial quantum number. The solution (47) is approximately correct if and only if the neglected terms are small compared to the terms that are kept. We estimate the value of the neglected terms at the turning points [which are the solution of $(1+x_t^2) = \epsilon_n/\sigma = (2n+1)/\sigma^{1/2}$ to be $g_0(1+x_t^2)^{-1} + (1+x^2)^{-2} \simeq g_0\sigma^{1/2}/(2n+1)$]. Thus the ratio of the neglected terms to the retained terms is $g_0/(2n+1)^2$ and becomes much smaller than unity for very large n numbers. Thus, the dispersion relation Eq. (47) is correct strictly in the large n limit. The eigenvalue turns out to be independent of g_0 because for very high n, the structure of the potential near $x = 0$ is quite unimportant. Another interesting feature is that the eigenvalue scales as $\sigma^{1/2}$, which makes high n modes relatively strongly damped. In addition, the damping increases with increasing n.

The main analytic results of this solution are: 1) Eqs. (39) and (35) describing the mildly damped lowest radial eigenmode of the GAE variety, with its characteristic frequency below the boundary of the MHD shear Alfvén continuum ($F = 0$). The damping is clearly a function of the model for parallel electron dynamics, 2) Eqs. (43) and (44), which describe the comparatively strongly damped lowest eigenmode of the discrete spectrum of what was the Alfvén continuum ($F \geq 0$). The damping of the mode seems to be quite insensitive to the model for parallel electron dynamics, 3) Eq. (47), which is the dispersion relation for very high ($n \gg 1$) radial mode numbers, and is independent of g_0. The damping rate increases with increasing n, and is essentially independent of the model of electron dynamics.

3 Compressional Waves

Section 2 was devoted to the shear Alfvén wave—the branch of the Alfvén spectrum which reduces to $\omega = k_\parallel v_A$ for a homogeneous infinite plasma. We found that the shear Alfvén spectrum, even for an axially and azimuthally symmetric equilibrium, was rich and varied. It is legitimate, then, to question why do we still persist in assigning the same generic name to such distinct entities like the Global Alfvén Eigenmodes (GAE), and the kinetic Alfvén waves (the discretized MHD continuum). The answer has been given by the consideration of Sec. 2, where we find that the dispersion relation for all these distinct cases does not depart significantly from $\omega = \left\langle \overline{k_\parallel v_A} \right\rangle$; where $\left\langle \overline{k_\parallel v_A} \right\rangle$ denotes the value of $k_\parallel v_A$ at the central location around which the mode is localized. This happens despite the fact that inhomogeneities couple the shear and the compressional wave. The coupling, in fact, does change the qualitative nature of the shear mode but still does leave the fundamental characteristics of the wave intact.

Because of this ruggedness of the dispersion relation, the shear Alfvén waves' phase velocity v_p (along the magnetic field) is wedded to the Alfvén speed v_A. This restriction might render the shear wave unsuitable for some applications. In order to efficiently drive a noninductive current in toroidally confined hot plasmas, for example, high phase speed [$v_p > v_e$, the electron thermal speed] waves are needed. The shear Alfvén with $v_p = v_A$ could not perform this function because in a typical hot plasma $v_e \gg v_A$. In the Alfvén wave literature, the inequality $v_e > (<) v_A$ defines a hot (cold) plasma; the transverse propagation of the wave is fundamentally different in the two regimes.[9]

Thus for a high phase speed current drive, below the ion cyclotron frequency, one must turn elsewhere. The compressional Alfvén wave turns out to be the candidate of choice. This section is devoted entirely to a delineation of the properties of the compressional Alfvén wave in a hot confined toroidal plasma (say, that of a tokamak reactor).

3.1 General Considerations

The theory of compressional waves[22–29] can become complicated due to the possibility of a strong coupling to the shear wave. In this paper we investigate compressional Alfvén waves with small toroidal mode numbers and frequencies below the ion cyclotron frequency as vehicles for heating and current drive in thermonuclear plasmas. Noting that the frequency range may be chosen to remove the shear Alfvén spatial resonance from the region between the plasma interior and the antenna,[28] we find analytical expressions for the spatial structure, frequency spectrum, and damping rates of eigenmodes corresponding to high-Q resonant absorption in a diffuse cylindrical plasma column. As mentioned earlier, the large parallel phase velocities of these modes make them attractive candidates for current drive.

Before proceeding with our analysis, it is worthwhile pointing out that several authors have investigated the low phase speed compressional waves when the two waves are strongly coupled. In Refs. 24 and 25 in particular, the authors, investigating tokamak plasmas, have focused their attention on cases in which $k_\parallel > k_\perp$, and the compressional and the shear mode are strongly coupled, i.e., the Alfvén resonance layer is close to the compressional wave cutoff. This happens when the toroidal mode number $l \gg m/q$, where m is the poloidal mode number, $q = rB_T/RB_p$ is the safety factor, B_T and B_p are the toroidal and the poloidal magnetic fields, and R is the major radius. In this limit, the compressional wave tends to be more strongly damped by absorption at the Alfvén resonance layer than by direct Landau or transit time magnetic pumping in the interior, typically leading to unacceptable absorption in the plasma edge region, just inside the antenna.

We show here, that in the opposite limit $k_\perp \gg k_\parallel$ (which implies $m \gtrsim l$) it is possible to have localized eigenmodes of the compressional wave which are not affected by the shear Alfvén wave. We do this by noting that the plasma edge density n_a is typically 2-5% of the central density and that the frequency may be chosen to exceed $k_\parallel v_A$ at the edge

and throughout the column, and still maintain $\omega \ll \omega_{ci}$. We first determine the dispersion relation for the discrete spectrum within the framework of magnetohydrodynamic equations. Then, we estimate the Landau and transit time magnetic damping of these modes using a perturbation theory. This calculation is similar in spirit to the earlier work of Perkins, who assumed $\omega \cong \omega_{ci}$, however. The principal result is that these modes are weakly damped, and the damping comes principally from the high temperature regions nearest the plasma center. That is, the wave loses energy to particles with high parallel speed. These are precisely the conditions for the suitability of a wave for generating current in the plasma.

Although the calculation is carried out for a tokamak plasma, treated as a cylinder of length $2\pi R$, the analysis is quite general to describe most cylindrical plasma systems.

3.2 Compressional Wave Spectrum in Magnetohydrodynamics

For the modes we are considering it is adequate to use the ideal magnetohydrodynamic equations without the effects of equilibrium current, its gradients, or finite ω/ω_{ci} corrections. It may be noted that for large tokamaks (reactor size) with density $n_0 \sim 10^{14}$, $\omega/\omega_{ci} \sim (m/r)v_A/\omega_{ci} < 1$ even for m numbers as large as ten. Finite ω/ω_{ci} and equilibrium current effects can be treated perturbatively, but in this paper, we restrict ourselves to the leading order problem.

We begin with the simpler and complete version of Eqs. (6)–(7) $[\omega/\omega_{ci} = 0,\ A = 0]$

$$\left(\frac{\omega^2}{v_A^2} - k_\parallel^2 - k_\perp^2\right) E_r = i\,\frac{k_\perp}{r}\,\frac{d}{dr}\,rE_\perp, \tag{48}$$

$$\left(\frac{\omega^2}{v_A^2} - k_\parallel^2 + \frac{d}{dr}\,\frac{1}{r}\,\frac{d}{dr}\,r\right) E_\perp = i\,\frac{d}{dr}\,k_\perp E_r, \tag{49}$$

where $k_\parallel \cong (-lq + m)/qR$, $k_\perp \cong m/r$, and all other symbols have their standard meaning. For an analysis of the compressional wave, it is more convenient to introduce a new variable

$$Y = \left[\frac{\left(\omega^2/v_A^2 - k_\parallel^2\right)}{k_\perp}\right] E_r \equiv \left(\frac{F}{k_\perp}\right) E_r,$$

which satisfies the differential equation

$$\frac{d}{dr}\frac{r}{F}\frac{dY}{dr}+r\frac{F-k_\perp^2}{F}Y=0. \tag{50}$$

Equation (49) can be further changed to a Schrödinger-like equation

$$\psi''+\left\{\frac{\omega^2}{v_A^2}-k_\parallel^2-\frac{m^2}{r^2}-\frac{1}{2}\left(\frac{F}{r}\right)^{1/2}\left[\left(\frac{F}{r}\right)^{1/2}\left(\frac{r}{F}\right)'\right]'\right\}\psi=0, \tag{51}$$

in the new variable

$$\psi=\left(\frac{r}{F}\right)^{1/2}Y=\left[\frac{(rF)^{1/2}}{k_\perp}\right]E_r, \tag{52}$$

where a prime denotes differentiation with respect to r.

Notice that $F=0$ is the shear Alfvén singularity. If this singularity falls in the region between the antenna and the plasma, then the structure of the compressional wave becomes complicated.[24-26] Typically, the antenna for the radio frequency current drive and heating experiments is placed in the shadow of the limiter, where the plasma density is 2-5% of the central density. Thus the Alfvén velocity at the antenna $v_A^a=5-7v_0$, where v_0 is the Alfvén speed at the plasma center. We show later that the spectrum for the compressional Alfvén waves is $\omega=[2(m+1+2n)v_0/r_0]$, where r_0 is the minor radius of the tokamak, and n is the radial mode number. Thus as long as $\omega>k_\parallel v_A^a$, that is $2(m+1+2n)>7r_0k_\parallel$, the shear Alfvén resonance does not lie in the region of interest. For an aspect ratio $R/r_0=3$, the above condition is easily satisfied for $m>l$.

Within the context of above discussion, we approximate $F\simeq\omega^2/v_A^2$. It is straightforward to see that the last term in the coefficient of ψ in Eq. (4) is a small cylindrical correction, and can be neglected compared to m^2/r^2 for moderate values of m. With these simplifications, the mode equation becomes

$$\frac{d^2\psi}{dr^2}+\left[\frac{\omega^2}{v_0^2}\left(1-\frac{r^2}{r_0^2}\right)-\frac{m^2}{r^2}\right]\psi=0, \tag{53}$$

where we have assumed a parabolic density profile $n=n_0(1-r^2/r_0^2)$. Equation (6) can be readily analyzed as a Whittaker equation, and has an exact solution whose finiteness at

the origin, and an appropriate boundary condition at $r = r_0$ will determine the eigenvalue as well as the eigenfunction. Although extremely suitable for this particular density profile, this method does not have a general validity. Instead, we follow an alternative approach, which makes the analysis physically more perspicuous, and can deal with arbitrary density profile.

The eigenmode equation is a Schrödinger-like equation

$$\psi'' + [\epsilon - V(r)]\psi = 0 \tag{54}$$

with $\epsilon = \omega^2/v_0^2$ as the effective energy, and

$$V(r) = \epsilon \frac{r^2}{r_0^2} + \frac{m^2}{r^2} \tag{55}$$

as the effective potential, which has a minimum at

$$r_{\min} = r_0 \left(\frac{m^2}{r_0^2 \epsilon}\right)^{1/4}. \tag{56}$$

Notice that the potential well is provided by a combination of the monotonically decreasing density and the fact that $k_\perp = m/r$ is a strongly varying function of r. Exploitation of this strong radial dependence of $k_\perp$ is an integral part of this analysis, for the modes are consequently confined to annular regions away from $r = 0$, rather than filling the whole plasma volume as is frequently assumed.

To obtain a spectrum for the eigenmodes localized in the potential well, we simply expand $V(r)$ around $r_{\min}$, define $x = r - r_{\min}$, and rewrite Eq. (53) in the form

$$\frac{d^2\psi}{dx^2} + \left[\left(\epsilon - 2\epsilon^{1/2}\frac{m}{r_0}\right) - \frac{4\epsilon}{r_0^2}x^2\right]\psi = 0, \tag{57}$$

which is the equation of a simple harmonic oscillator. For the boundary conditions $\psi \to 0$ as $x \to \infty$, Eq. (56) allows the spectrum of eigenfunctions

$$\psi_n = 2^{-n/2} H_n\left[(4\epsilon_n)^{1/4}\frac{x}{r_0}\right] \exp\left(-\frac{\epsilon_n^{1/2}}{r_0}x^2\right) \tag{58}$$

and the associated eigenvalues

$$\omega_n = \epsilon_n^{1/2} v_0 = 2(m + 1 + 2n) v_0 / r_0, \tag{59}$$

where n is the radial mode number, and H_n are the Hermite polynomials. Using a variational method, Perkins obtained a somewhat different result for the fundamental ($n = 0$) mode when $\omega = \omega_{ci}$.

Making use of Eqs. (55) and (59), we find that

$$\frac{r_{\min}}{r_0} = \frac{1}{\sqrt{2}} \left(\frac{m}{m + 1 + 2n} \right)^{1/2}. \tag{60}$$

For a given m number, $r_{\min}$ shifts towards the plasma center as the radial mode number n increases. Thus a suitable choice of m and n allows us to center the mode wherever we desire. The turning points of the system are given by Eqs. (56) and (57) to be

$$\frac{x_t^2}{r_0^2} = \frac{(r - \min)^2}{r_0^2} = \frac{1}{4} \frac{2n + 1}{2n + 1 + m}, \tag{61}$$

implying that for $n > m$, the inner turning point tends to approach the plasma center, while the outer turning point approaches the plasma edge. In this limit, the results derived in this paper are expected to be only approximately correct. It turns out, however, that the exact Eq. (52), when solved as a Whittaker equation, yields essentially the eigenvalue given in Eq. (58).

We have shown that in a magnetically confined cylindrical plasma, localized eigenmodes of the compressional Alfvén wave exist in the potential well provided by the radial variation of plasma density (which changes the Alfvén speed), and the perpendicular mode number $k_\perp = m/r$. We have also determined the spectrum of eigenvalues. For current drive experiments, these modes must be connected to the antenna; this question will not be addressed in this review. Detailed numerical work, however, has demonstrated extremely efficient coupling. In addition, the theoretically derived mode structure closely resembles the numerical results.

One must also calculate the damping rates before a realistic estimate of the usefulness of these modes for practical applications can be made. The damping calculations are rather detailed and involved and the reader should consult the original sources.[22–29] Schematically, the principal damping mechanisms (Landau damping and Transit Time Magnetic pumping) modify the mode Eq. (52) to

$$\frac{d^2\psi}{dr^2} + \left[\frac{\omega^2}{v_0^2}\left(1 - \frac{r^2}{r_0^2}\right)(1+b_i)^{-1} - \frac{m^2}{r^2}\right]\psi = 0 \tag{62}$$

where b_i is imaginary. Letting $(1+b_i)^{-1} \cong 1 - b_i$, expanding around $r_{\min}$, and applying a standard perturbation theory, we obtain the damping

$$\frac{\delta\omega}{\omega} = \frac{\frac{1}{7}2\int_{-\infty}^{\infty} dx b_i(1 - r^2/r_0^2)\psi^2}{\int_{-\infty}^{\infty} dx(1 - r^2/r_0^2)\psi^2}. \tag{63}$$

Notice that $b_i = i\pi^{1/2}(\omega/k_\parallel v_e)\exp(-\omega^2/k_\parallel^2 v_e^2)$ is maximum and of order unity for $\omega = k_\parallel v_e$. Because of the large phase velocity $v_p = \omega/k_\parallel$ of the waves under consideration, there is a comparatively larger contribution to damping from the inner regions of the plasma where v_e is large, i.e., the temperature is high. More quantitatively, the maximum wave-particle resonance condition is $v_e = \omega/k_\parallel \cong 2v_0(m+1+2n)/(k_\parallel r_0)$. For typical wave numbers of interest $m = 2, l = 1, n = 0$, and an aspect ration $R/r_0 = 3$, the preceding condition becomes $v_e/v_0 = 18$. For a reactor plasma at 10 KeV, density $\sim 5 \times 10^{14}, B_0 \sim 50$ Kg, $v_e/v_0 \sim 10$ implying significant wave particle coupling near the plasma center. It can be seen from Eq. (25) that even when $\omega \simeq k_\parallel v_e$, Im $\omega/\omega \simeq 0.2\beta_e \simeq 10^{-2}$ for typical reactor parameters.

We must now distinguish between two possible applications of the compressional waves. For plasma heating, we need to maximize P_d, the power dissipated. This is attained by maximizing the wave-particle coupling, which happens if the mode numbers are so chosen that $\omega \simeq k_\parallel v_e$ in the plasma interior. For current drive applications, however, one needs to optimize J/P_d (J is the current generated). This ratio becomes large if $v_p = \omega/k_\parallel > v_c$, and would, in general, require a different choice of mode numbers. The particular numbers

chosen will depend upon the plasma conditions. It should be mentioned that current drive becomes efficient also for low phase velocity $v_p < v_e$. But in this case, it is difficult to avoid the shear Alfvén resonance in the plasma which often leads to unacceptable absorption in the plasma edge region.

We end this section by making a comment on the relative magnitudes of the mode numbers l, m and n. The primary consideration is to assure that $\omega/k_\parallel > v_A$ everywhere in the plasma to avoid the shear Alfvén resonance. Since ω is determined by a combination of m and n numbers, this can be readily satisfied if $m + 2n + 1 \geq l$ for typical discharges [see discuss Eq. (51)]. Thus low m numbers like $m = 2$ are adequate if $l = 0$ or 1. Although, it is difficult to justify neglecting cylindrical corrections in Eq. (50) for such low m numbers, we find by extensive numerical solutions using the code of Ref. 9 that our analytical results are correct within a few percent.

3.3 Summing Up Compressional Waves

In addition to its inherent scientific value, the knowledge of the spectrum of compressional cavity modes, thus, guides us as to how to choose the defining labels in order to optimize their utility for a given practical application. The compressional eigenmode seems to be very mildly damped implying its high-Q nature. Thus large fields can be built up with an external antenna; the plasma simply acts like an amplifier. Since the dissipation process is effective only for high speed particles because of the relatively large parallel phase velocity $v_p \sim \omega_0/k_\parallel$, this mode is ideally suitable for radio frequency current drive, which becomes more and more efficient as v_p exceeds v_e. Thus by a suitable choice of m and n we can adjust the value of v_p/v_e for a given plasma, and optimize the conditions for current drive. Because of the low $k_\parallel$, this mode should not have accessibility problems, because we have already shown that in the region near the plasma edge where temperature is relatively low, the Landau process is extremely weak, and of no importance. In this region, collisional

damping, perhaps will be more important.

4 Two-Dimensional Waves—Gap Modes

Till recently, much of the stable Alfvén wave literature was limited to cylindrically symmetric equilibria. But a recent realization, that a new kind of Alfvén mode (which owes its origin to the two-dimensional character of the ambient magnetic mode) could be important in a thermonuclear-reactor plasma, has excited considerable interest in the two-dimensional (2D) Alfvén waves. Although the impetus for studying 2D waves comes from fusion physics, these waves are likely to be present in all kinds of space and astrophysical plasmas; their investigation, therefore, is of general interest.

Analysis presented in the preceding sections clearly indicates that theory of Alfvén waves tends to get quite complicated even when the plasma inhomogeneity is limited to one direction. Along with this complexity, of course, comes the possibility of enriching the wave-spectrum, even, qualitatively changing the nature of the spectrum.

It is natural to expect that addition of a new direction of inhomogeneity will further complicate as well as enrich the class of wave motions sustained by the plasma. To simulate many of these situations, we shall now allow the equilibrium magnetic field to have, in addition to a 'radial' dependence, a periodic variation in an azimuthal angle θ. The eigenvalue problem is fully two dimensional, and would generally require sophisticated numerical methods for a solution. In this review, however, we will present a model example which illustrates the new features pertaining to the second dimension of inhomogeneity, but avoids complications.

The principal change brought about by the inhomogeneity in θ is that θ, though a periodic variable, is no more ignorable. Thus the standard expansion of the fluctuating quantities, $\phi \sim \sum_m \phi_m e^{im\theta}$ (still allowed by the periodicity in θ) does not lead to independent decoupled equations for the amplitudes ϕ_m, i.e. m is not a good quantum number. Thus the two-dimension (2D) eigenmode must be constructed by an appropriate superposition of ϕ_m's.

Under certain special conditions, this superposition can lead to the creation of square integrable normal modes,[30-43] which have no counterpart in a plasma homogeneous in θ. These gap modes, generally referred to as Toroidal Alfvén Eigenmodes (TAE), are a subject of active investigation.

To understand the origin of these new modes, we go back to our standard axisymmetric low aspect ratio torus, an excellent representative of the physical systems under consideration. To motivate the 2D theory, we must review the simple 1D theory. We remind the reader that the toroidal angle $\xi \cong z/R_0$ (R_0 is the major radius of the torus), the poloidal angle θ, and the radial variable r, define an approximate orthogonal set of coordinates. The ambient magnetic field is still of the form,

$$\mathbf{B}_0 = B_z \hat{e}_z + B_\theta \hat{e}_\theta \tag{64}$$

with both B_z and B_θ independent of z (axisymmetry). Any perturbation then, can still be expanded as

$$\phi = \phi_n e^{inz/R_0} \tag{65}$$

implying that the all important operator $k_\parallel = \mathbf{b} \cdot \boldsymbol{\nabla} = (B_z/|\mathbf{B}_0|)R_0^{-1}\left[i\ell + q^{-1}\,\partial/\partial\theta\right]$, where $q = rB_z/R_0B_z$ is the standard MHD safety factor. If the equilibrium were further independent of θ, then the expansion $\phi_m = \phi_{nm}e^{-im\theta}$ would lead to independent modes ϕ_{nm} with the local dispersion relation [equivalent to $d(\omega, k, n)$]

$$\hat{\omega}_m^2(r) = k_\parallel^2(r)v_A^2(r) = v_A^2\,R_0^{-2}\left[n - \frac{m}{q(r)}\right]^2, \tag{66}$$

leading to the continuous spectrum because of the singularity $\hat{\omega}^2(r) = \omega^2$. A few typical dispersion relations are plotted in Fig. 3. Now suppose that we introduce a θ dependent perturbation to the equilibrium, then for a given n (still a good quantum number), various m numbers will couple, i.e. the local dispersion relations for various m modes will interact. Now if at some location $r = r_0$, $\hat{\omega}_{m1}^2$, and $\hat{\omega}_{m_2}^2$ were to coincide, then the coupling of these

(m_1 and m_2) modes will be very strong even for a very small perturbation. Notice that such a situation pertains if $(n - m_1/q = -(n - m_2/q)$, i.e. if $m_2 + m_1 = 2nq(r_0)$. At $r = r_0$, then, the two interacting dispersion curves $\widehat{\omega}^2_{m_1}(r)$ and $\widehat{\omega}^2_{m_2}(r)$ are split by the perturbation giving rise to a gap proportional to the strength of the perturbation [Fig. 4]. Clearly an ω^2 lying in the gap cannot ever equal $k^2_\parallel v^2_A$, the differential equation for the Alfvén wave is no more singular, and a discrete 'gap' mode appears. This is a qualitatively new feature introduced by the two-dimensional character (coupling of m modes) of the plasma equilibrium. These gap modes are widely discussed in literature.

The careful reader must have guessed by this time that these gaps that appear in the continuous spectrum of Alfvén waves are very similar to the energy gaps in the spectrum of an electron moving in the periodic potential of a crystal lattice. In fact, in the model problem that we will solve in this section, the analogy will become totally transparent.

We continue with our problem of Alfvén waves in an axisymmetric torus. Let us assume, for simplicity, that the θ dependence of the equilibrium stems only from the weak dependence of the magnetic field $B_z \sim B_0(1 + \epsilon\cos\theta)^{-1} \simeq B_0(1 - \epsilon\cos\theta)$ where $\epsilon < 1$. Because of the weakness of the θ dependence, we still go ahead and expand

$$\phi_n = e^{im\theta}\sum_\ell e^{i\ell\theta}\phi_{n\ell} \equiv e^{im\theta}\sum_\ell e^{i\ell\theta}\phi_\ell \tag{67}$$

where m is some central mode number around which the mode is localized in the m space, i.e. the spread measured by $\ell \ll m$, the basic mode number. The 2D problem is much better handled by using the scalar potential ϕ instead of the electric fields. Using (67), the basic MHD equations can be manipulated, and after some straightforward but tedious algebra[42–43] the Alfvén wave equation can be put in the schematic form (see (42) for details)

$$\frac{d}{dx}\left[\Omega^2\frac{f(x)}{4} - (x-\ell)^2\right]\frac{d\phi_\ell}{dx} - \frac{1}{s^2}\left(\frac{\Omega^2 f(x)}{4} - (x-\ell)^2\right)\phi_\ell$$
$$+\epsilon\frac{\Omega^2}{4}\left[\frac{d^2\phi_{\ell+1}}{dx^2} + \frac{d^2\phi_{\ell-1}}{dx^2}\right] = 0 \tag{68}$$

where the effective radial variable $x = n\ (q - q_0)$ measure the distance from r_0 defined by $q(r_0) = m/n$. In Eq. (75), $\Omega = \omega/\omega_A$, is the mode frequency normalized to the Alfvén frequency at r_0 ($\omega_A = (k_\parallel v_A)r = r_0$), $s = (d\ell n\, q/d\ell n\, r)_{q=q_0}$ is the magnetic shear, $f(x)$ represents the radial variation of the Alfvén frequency, and ϵ measures the strength of the θ dependent corrections to the equilibrium.

Equation (68) is clearly two dimensional: the independent coordinates are the continuous variable x, and the discrete variable ℓ. As such, it is difficult to make further analytical progress, even with this model equation. Since the aim of this review is to introduce the reader to the broad generic classes of spectra that Alfvén waves can display, we will deal here with the simplest illustrative example.

Let $f(x) \equiv f_0$ be a constant. In this case Eq. (68) can be reduced to an effective one-dimensional equation; this enormous simplification emerges from the realization that Eq. (68) is invariant under the translation $x \to x + 1, \ell \to \ell + 1$.

It should be emphasized that this translational invariance (also called the ballooning symmetry) of the leading order equation allows the possibility of developing a systematic procedure for constructing an asymptotic theory in the more general case when $f(x)$ is not a constant.[42]

Let us introduce a 2D Fourier transform[42]

$$\phi_\ell(x) = \oint d\lambda \int dk\, \exp[ik(x - \ell) - i\lambda\ell]\widehat{\phi}(k, \lambda) \tag{69}$$

where k is the conjugate of $x - \ell$, and λ that of ℓ; λ is periodic. Using Eq. (69), and defining

$$\phi = \widehat{\phi}(1 + s^2k^2)^{1/2}, \tag{70}$$

Eq. (68) becomes [$\Omega^2 f(x) = \Omega^2 f_0 = 1 + \epsilon g$]

$$\frac{\partial^2}{\partial k^2}\,\phi(k, \lambda) + \left[\frac{1 + \epsilon g}{4} - \frac{s^2}{(1 + s^2k^2)^2} + \frac{\epsilon}{2}\cos(k + \lambda)\right]\phi(x, \lambda) = 0 \tag{71}$$

which is a one-dimensional equation parameterized by λ, and with g as the effective eigenvalue. But for the term $s^2/(1+s^2k^2)^2$, representing a repulsive potential centered at $k=0$, Eq. (71) is nothing but a Mathieu equation; precisely the type of equation obeyed by an electron in a periodic crystal lattice. Although neither term of the effective potential, $s^2/(1+s^2k^2)^2$ or $\cos(k+\lambda)$ is capable of yielding square integrable localized eigenfunctions, their combination, in fact, does yield discrete modes in the gap.[42,43]

In this simple case, the spectrum g turns out to be purely real as expected from (71). Thus, it is possible, to obtain a point spectrum in two dimensions, the one-dimensional singularity of each m mode becomes obviated by the coupling and interaction of many m modes.

We have given a very short summary, and picked up a simple illustrative example, to convey the spectral essence of the two-dimensional Alfvén waves. For further details, viz., the continuum or kinetic damping of these gap modes, the details of destabilizing mechanisms (like the fusion generated fast particles), the nonlinear saturation of these modes (primarily by the mode's ability to weaken the drive), the reader is encouraged to survey the vast body of available literature.[30–43]

5 Summary

The aim of this modest review was to give a glimpse of the richness of the Alfvén wave physics. In confined, hot plasmas, Alfvén waves take extremely interesting and varied forms with the leading order structure dictated by the magnetic field geometry. When the magnetohydrodynamic description leads to singular modes, the electron kinetic effects regularize, and therefore, determine the structure of the mode. Although we have limited ourselves, here, to a theory of the spectral aspects of the waves, it must be emphasized that several experimental attempts, with very promising results,[44] have been made to map out the spectrum of the Alfvén waves. However, this vast and exciting field is still rather unexploited

and beckons enterprising experimentalists. Similarly, the theory of high amplitude waves (nonlinear GAE, KAW, or TAE), in spite of a few important advances,[45–46] defines a difficult and challenging field for investigation. We must also note that additional structure of the ambient magnetic field (no symmetry, no ignorable dimension) introduces altogether new and unknown features[47] to the physics of Alfvén waves; it is a plum ready to be picked.

The branch of physics born with Hannes Alfvén has had a glorious past. With the breadth and depth of problems still waiting to be solved, the future has to be even brighter.

References

1. H. Alfvén, On the existence of electromagnetic-hydrodynamic waves, Arkiv. Mat. Astron. Fysik B **29**(2) (1942);

   H. Alfvén, *Cosmical Electrodynamics*, (Oxford University Press, New York, 1950).

2. H. Grad, Phys. Today **22**, 34 (1969);

   H. Grad, Proc. Nat. Acad. Sci. **70**, 3277 (1993).

3. C. Uberoi, Phys. Fluids **15**, 1673 (1972).

4. J.P. Goedbloed, Phys. Fluids **18**, 1258 (1975).

5. E. Hamieri, Comm. Pure Appl. Math. **38**, 1258 (1975).

6. T. Kako, Math. Mech. Appl. Sci. **7**, 432 (1985).

7. A. Hasegawa and C. Uberoi, The Alfvén wave, DoE Critical Rev. Series, DoE/TIC-11197 (Technical Information Center, U.S. Department of Energy, Springfield, 1982).

8. For a recent review, see J. Vaclavic and K. Appert, Nucl. Fusion **31**(10), 1945 (1993).

9. D.W. Ross, G.L. Chen, and S.M. Mahajan, Phys. Fluids **25**, 652 (1982).

10. S.M. Mahajan, D.W. Ross, and G.L. Chen, Phys. Fluids **26**(8), 2195 (1983).

11. S.M. Mahajan, Phys. Fluids **27**(9), 2234 (1984).

12. K. Appert, R. Gruber, F. Troyon, and J. Vaclavik, in *Proceedings of the 3rd Joint Varenna-Grenoble International Symposium*, Grenoble, 1982 (ECSC-EEC-EAEC Euratom, Brussels, 1982), Vol. 1, pp. 203-212.

13. K. Appert, R. Gruber, F. Troyon, and J. Vaclavik, Phys. Plasmas **24**, 1147 (1982).

14. A. de Chambrier, A.D. Cheetham, A. Heym, F. Hofmann, B. Joye, R. Keller, A. Lietti, J.B. Lister, A. Pochelon, A. Simm, J.L. Toninato, and A. Tuszel, in *Proceedings of the 3rd Joint Varenna-Grenoble International Symposium*, Grenoble, 1982 (ECSC-EEC-EAEC Euratom, Brussels, 1982), Vol. 1, pp. 161-172.

15. See for example, W. Grossman and J. Tataronis, Z. Phys. **261**, 217 (1973); and J.P. Goedbloed, Phys. Fluids **18**, 1258 (1975).

16. K. Appert, B. Balet, R. Gruber, F. Troyon, T. Tsunematsu, and J. Vaclavik, Phys. Lett. A **87**, 233 (1982).

17. Y.P. Pao, Nucl. Fusion **14**, 25 (1974).

18. J.A. Tataronis and W. Grossman, Z. Physik **261**, 203 (1973).

19. K.N. Stepanov. Sov. Phys. JETP **34**, 895 (1958).

20. K.J. Stefant, Phys. Fluids **13**, 440 (1970).

21. A. Hasegawa and L. Chen, Phys. Rev. Lett. **32**, 454 (1974).

22. F.W. Perkins, in *Proceedings of the Symposium on Plasma Heating and Injection*, Varenna, Italy, 1972 (Editrice Composotori, Bologna, 1973), p. 20.

23. T.M. Stix, Nucl. Fusion **15**, 737 (1975).

24. E. Ott, J.M. Wersinger, and P.T. Bonoli, Phys. Fluids **21**, 2306 (1978).

25. C.F.F. Karney, F.W. Perkins, and Y.C. Sun, Phys. Rev. Lett. **42**, 1621 (1979).

26. F.W. Perkins, Bull. Am. Phys. Soc. **27**, 1101 (1982).

27. See, for example, N.J. Fisch, Phys. Rev. Lett. **41**, 873 (1978).

28. S.M. Mahajan and D.W. Ross, Phys. Fluids **26**, 2561 (1983).

29. Y.M. Li, S.M. Mahajan, and D.W. Ross, Phys. Fluids **30**(7), 2101 (1987).

30. C.Z. Cheng, L. Chen, and M.S. Chance, Ann. Phys. **161**, 21 (1985).

31. S. Riyopoulos and S.M. Mahajan, Phys. Fluids **29**, 737 (1986).

32. C.Z. Cheng and M. Chance, Phys. Fluids **29**, 3695 (1986).

33. G.Y. Fu and J.W. Van Dam, Phys. Fluids B **1**, 1969 (1989).

34. K.L. Wong, Phys. Rev. Lett. **66**, 1874 (1991).

35. W.W. Heidbrink, E.J. Strait, E. Doyle, and R. Snider, Nucl. Fusion **31**, 1635 (1991).

36. R.R. Mett and S.M. Mahajan, Phys. Fluids B **4**, 2885 (1992).

37. F. Zonca and L. Chen, Phys. Rev. Lett. **68**, 592 (1992).

38. M.N. Rosenbluth, H.L. Berk, J.W. Van Dam, and D.M. Lindberg, Phys. Rev. Lett. **68**, 596 (1992).

39. M.N. Rosenbluth, H.L. Berk, J.W. Van Dam, and D.M. Lindberg, Phys. Fluids B **4**, 2189 (1992).

40. H.L. Berk, J.W. Van Dam, Z. Guo, and D.M. Lindberg, Phys. Fluids B **4**, 1806 (1992).

41. H. Ye, Z. Sedlacek, and S.M. Mahajan, Phys. Fluids B **5**, 2999 (1993).

42. X.D. Zhang, Y.Z Zhang, and S.M. Mahajan, Phys. Fluids B **4**, 1257 (1993).

43. X.D. Zhang, Y.Z Zhang, and S.M. Mahajan, Phys. Plasmas **5**(2), 381 (1994).

44. T.E. Evans, R.D. Bengtson, D.W. Ross, P.M. Valanju, M.E. Oakes, and S.M. Mahajan, Phys. Rev. Lett. **53**, 1743 (1984), and references therein.

45. F. Brunel, J-N. Leboeuf, and S.M. Mahajan, Phys. Rev. Lett. **54**(12), 1252 (1985).

46. See for example, H.L. Berk, B.N. Breizman, and H.C. Ye, Phys. Rev. Lett. **68**(24), 3563 (1992); H.L. Berk, B.N. Breizman, and M. Pekker, Phys. Plasmas **2**(8), (1995), and references therein.

47. See for example, Z. Yoshida, Phys. Rev. Lett. **68**, 3168 (1992).

Figure Captions

1. $v(x)$ versus x for the MHD limit $\sigma = 0$. The curves have different values of $g_0 \equiv g$. Notice that $v(x) \to 0$ as $x \to \infty$ for all the curves.

2. $v(x)$ versus x for the dissipative case, $\sigma = 10^{-2}$. The potential well at large x is responsible for the discrete spectrum of the Kinetic Alfvén Wave (KAW).

3. The local Alfvén frequency $\widehat{\omega}^2 = k_\parallel^2 v_A^2(r)$ as a function of r for several azimuthal (poloidal) mode numbers m for a given axial (toroidal) mode number n. The increase away from the center is normally due to the decreasing density.

4. Gap formation due to the degeneracy, at some radial location, of the local Alfvén frequencies $\widehat{\omega}_{m_1}^2$ and $\widehat{\omega}_{m_2}^2$ corresponding to mode numbers m_1 and m_2.

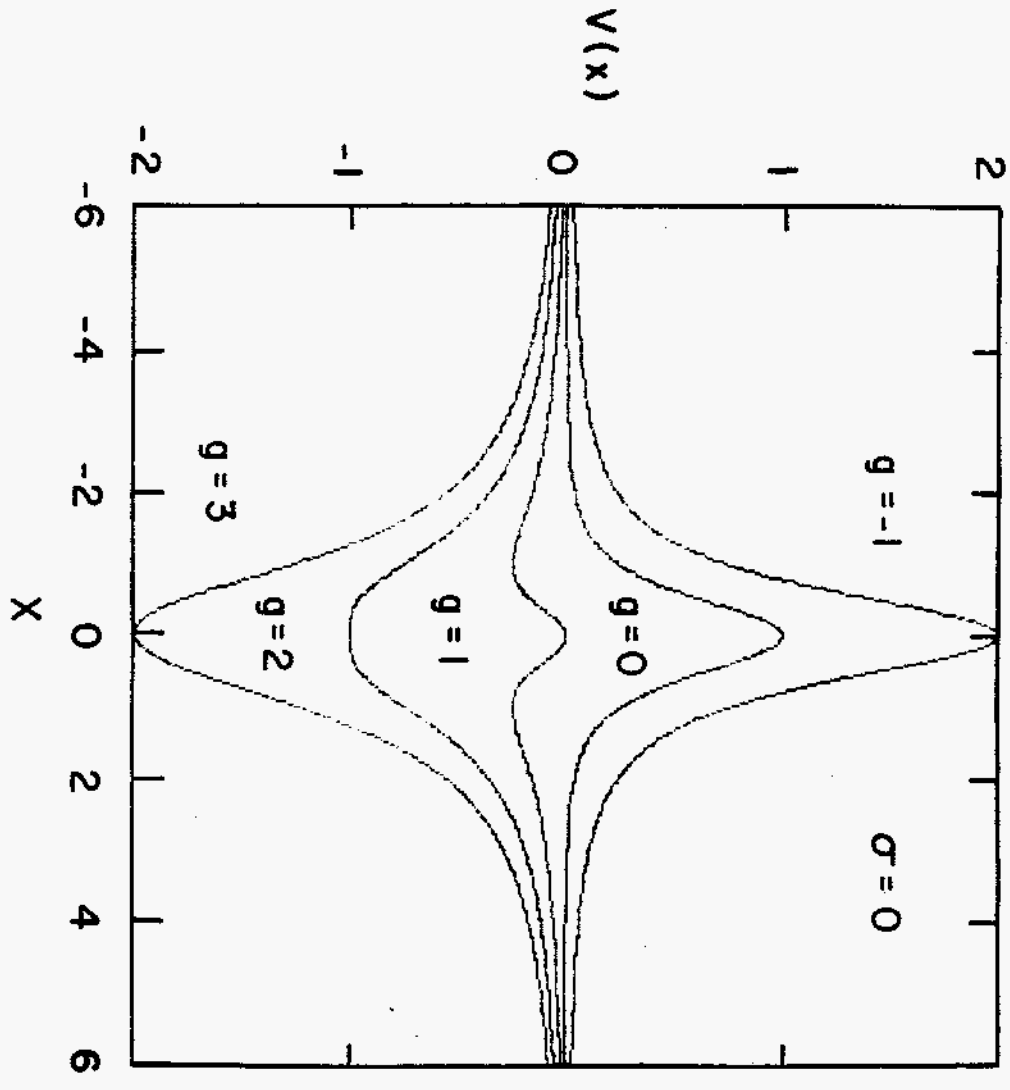

Fig. 1

Fig. 2

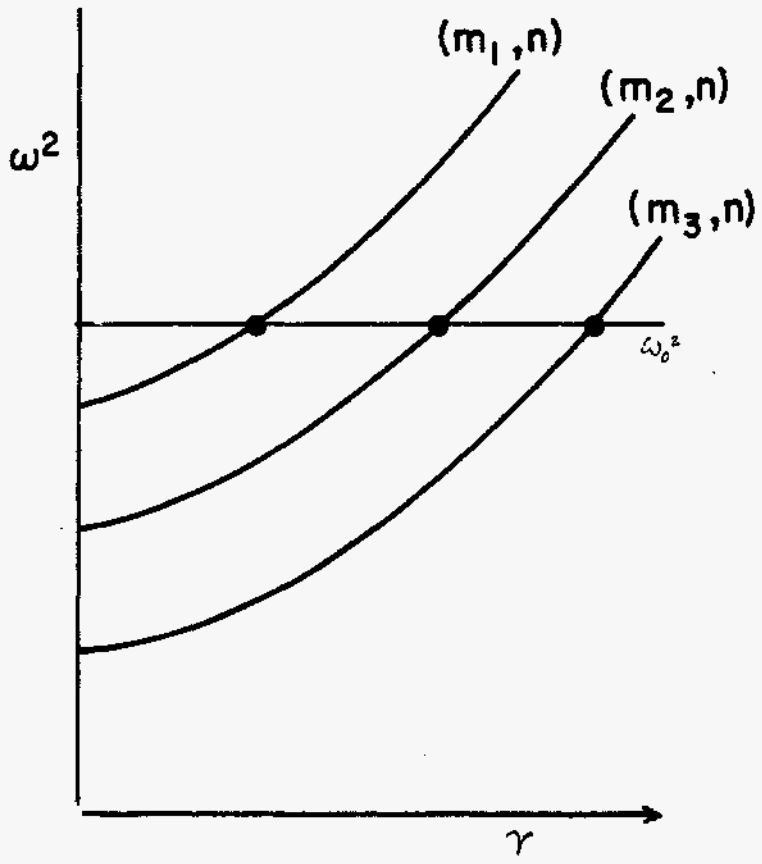

Fig. 3

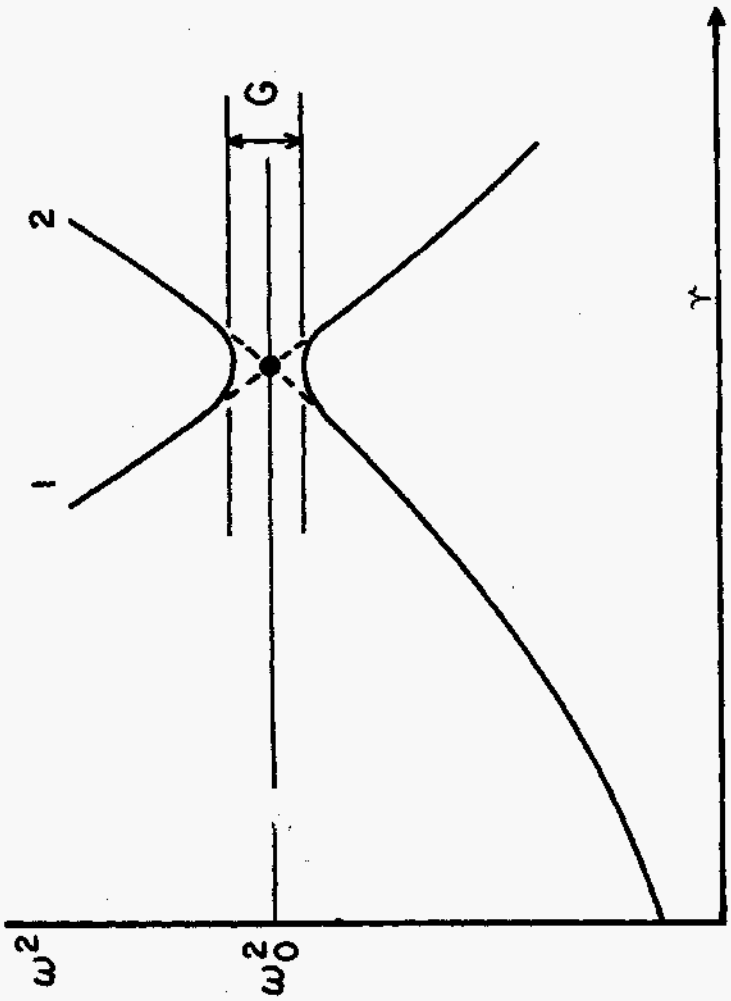

Fig. 4